Proposal for a Bosonic Cascade Laser

T. C. H. Liew,[1] M. M. Glazov,[2,3] K. V. Kavokin,[2,3] I. A. Shelykh,[1,4] M. A. Kaliteevski,[2,5] and A. V. Kavokin[3,6]

[1]*Division of Physics and Applied Physics, Nanyang Technological University, 637371 Singapore, Singapore*
[2]*Ioffe Phyical-Technical Institute of the RAS, 26, Polytechnicheskaya, St. Petersburg 194021, Russia*
[3]*Spin Optics Laboratory, St. Petersburg State University, 1 Ul'anovskaya, St. Petersburg 198504, Russia*
[4]*Science Institute, University of Iceland, Dunhagi-3, IS-107 Reykjavik, Iceland*
[5]*St. Petersburg Academic University, 8/3 Khlopina Street, St. Petersburg 194021, Russia*
[6]*University of Southampton, Highfield, Southampton SO17 1BJ, United Kingdom*

(Received 11 May 2012; revised manuscript received 15 November 2012; published 25 January 2013)

We propose a concept of a quantum cascade laser based on transitions of bosonic quasiparticles (excitons) in a parabolic potential trap in a semiconductor microcavity. This laser would emit terahertz radiation due to bosonic stimulation of excitonic transitions. The dynamics of a bosonic cascade is strongly different from the dynamics of a conventional fermionic cascade laser. We show that populations of excitonic ladders are parity dependent and quantized if the laser operates without an external terahertz cavity.

DOI: 10.1103/PhysRevLett.110.047402 PACS numbers: 78.67.Pt, 78.45.+h, 78.66.Fd

Quantum cascade lasers (QCLs) are based on subsequent intersubband transitions of electrons or holes in a Wannier-Stark ladder formed in a semiconductor superlattice subject to an external electric field [1–3]. Emitted terahertz (THz) photons are polarized perpendicularly to the plane of the structure and propagate in plane (which is referred to as wave guiding or horizontal geometry). QCLs differ from conventional lasers as they do not require an inversion of electronic population for every particular transition. Still, this is a fermionic laser, where the quasiparticles emitting light obey the Pauli principle. Recently, several proposals for bosonic THz lasers based on exciton polaritons have been published [4,5]. These sources are expected to generate THz light beams propagating in the normal-to-plane direction (vertically) without external THz cavities [6]. The emitted radiation is stimulated by the final state (exciton-polariton) occupation, which is a purely bosonic effect.

Here, we propose a concept of a bosonic cascade laser that combines the advantages of QCLs (emission of multiple THz photons for each injected electron) and exciton-polariton lasers (no need for a THz cavity, low threshold). We consider an exciton cascade formed by equidistant energy levels of excitons confined in a parabolic trap in a semiconductor microcavity. As shown below, in such a geometry, the most efficient THz transitions are possible between neighboring levels. Parabolic traps for exciton polaritons have been experimentally demonstrated, and an equidistant spectrum of laterally confined exciton-polariton states has been observed. There are several ways to realize such traps, including specially designed pillar microcavities [7], strain induced traps [8], and optically induced traps [9–11]. A particularly promising variation of these designs would be a microcavity with a large parabolic quantum well embedded. We consider the weak coupling regime where the optical mode is resonant with the mth exciton level to allow efficient pumping. The other energy levels of the confined excitons would be uncoupled to the cavity mode, forming a dark cascade ideal for a high quantum efficiency device due to the long radiative lifetime. This device would emit radiation polarized in the direction normal to the quantum well plane and propagating in the cavity plane in the wave guiding regime. In this Letter, we formulate a kinetic theory of bosonic cascade lasers and carry out a microscopic calculation of the transition rates and quantum efficiency of such a device. We show that the quantum efficiency is at least 3 orders of magnitude larger than previous designs based on stimulated emission [4] and several orders of magnitude larger than the corresponding fermionic cascade.

The occupation numbers of exciton quantum confined states and the THz optical mode in our cascade laser can be found from the following set of kinetic equations (0 is the state with the lowest energy, and m is the state with the highest energy, which is resonantly pumped):

$$\frac{dN_m}{dt} = P - \frac{N_m}{\tau} - WN_m(N_{m-1}+1) + W'N_{m-1}(N_m+1), \tag{1}$$

$$\frac{dN_k}{dt} = -\frac{N_k}{\tau} + W[N_{k+1}(N_k+1) - N_k(N_{k-1}+1)] + W'[N_{k-1}(N_k+1) - N_k(N_{k+1}+1)] \quad \forall\ 1 \le k \le m-1, \tag{2}$$

$$\frac{dN_0}{dt} = -\frac{N_0}{\tau} + WN_1(N_0+1) - W'N_0(N_1+1), \tag{3}$$

$$\frac{dn_{\mathrm{THz}}}{dt} = -\frac{n_{\mathrm{THz}}}{\tau_{\mathrm{THz}}} + W\sum_{1}^{m} N_k(N_{k-1}+1) - W'\sum_{1}^{m} N_{k-1}(N_k+1). \quad (4)$$

Here, $W = W_0(n_{\mathrm{THz}}+1)$ is the THz emission and $W' = W_0 n_{\mathrm{THz}}$ is the THz absorption rate, n_{THz} is the THz mode occupation, and τ_{THz} is the THz mode lifetime. The lifetime of the cascade levels, τ, should include both their radiative lifetime and their nonradiative lifetime, which includes losses due to phonon scattering to states with a nonzero in-plane wave vector, $k_{\|} \neq 0$. Above a threshold pump power, it is not necessary to calculate explicitly the dynamics of these states. We note that any phonon or exciton-exciton scattering to $k_{\|} \neq 0$ states would not be stimulated, and any population in a particular subband can be expected to return to the $k_{\|} = 0$ state of the same subband by stimulated scattering. Phonon assisted relaxation between subbands is also expected to have a limited rate [12]. We assume that the matrix element of the THz transition is (i) nonzero only for neighboring stairs of the cascade and (ii) the same for all neighboring pairs. This simplifying assumption allows for the analytical solution of Eqs. (1)–(3). As we show below, condition (i) is approximately true for parabolic wells, while assumption (ii) can be easily relaxed in the numerical calculations.

We first consider the case where there is no THz cavity and assume that THz photons leave the system immediately such that $n_{\mathrm{THz}} = 0$. The solid curves in Fig. 1 show the dependence of the mode occupations on the pump power in this case, which were calculated by numerical solutions of Eqs. (1)–(3) for the steady state. For increasing pump power, we see that the modes become occupied one by one and that a series of steps appears, each corresponding to the occupation of an additional mode. In the limit $W_0\tau \ll 1$, the position of the steps is given by $P/W_0 = n^2/(W_0\tau)^2$, where n is a half-integer. For high pump powers, where all modes are occupied, two different behaviors of the modes can be identified: the zeroth, 2nd, 4th, etc. modes continue to increase their occupation with increasing pump power, while the 1st, 3rd, 5th, etc. modes have a limited occupation. This effect persists independently of whether an even or odd number of modes is considered in the system.

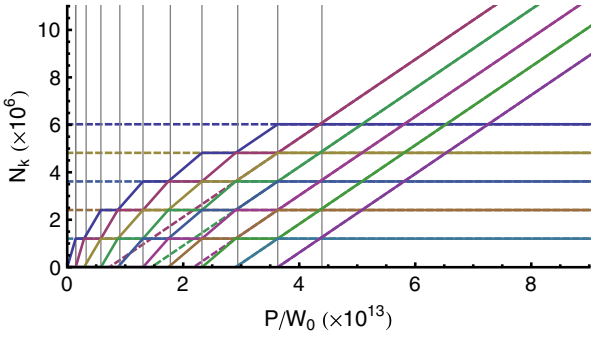

FIG. 1 (color online). Dependence of the mode occupations in the absence of a THz cavity on pump intensity, calculated numerically from the kinetic Eqs. (1)–(3) (solid curves) and analytically from Eqs. (5) and (6) (dashed curves). The vertical gray lines correspond to the step locations given by $P/W_0 = n^2/(W_0\tau)^2$, where n is a half-integer. The parameters are $W_0\tau = 8.3 \times 10^{-7}$, $m = 9$, and $n_{\mathrm{THz}} = 0$.

Qualitatively, our results can be understood as follows. Every mode in the chain experiences both a gain and a loss. The last mode in the chain is unique since it only experiences loss due to the finite lifetime rather than THz emission. Since it experiences loss only due to the lifetime, we can expect that the last mode is strongly occupied in the limit of high pump power. This means that the second-to-last mode experiences a strong loss due to stimulated scattering to a highly occupied state. Thus, the second-to-last mode has a much smaller occupation. The third-to-last mode then experiences only a small loss due to stimulated scattering and so can again have a large occupation. The series repeats such that alternate modes have high and low intensity, with the highly occupied modes introducing a fast loss rate that limits the occupation of low intensity modes.

Quantitatively, Eqs. (1)–(3) can be solved analytically in the steady state, where $\sum_k N_k = P\tau$, under the assumption that $W_0\tau \ll 1$, $N_m \gg 1$, and $n_{\mathrm{THz}} = 0$. In this regime, N_0 and the populations of modes with even indices grow linearly with the pump intensity [13]:

$$N_{2l} = N_0 + \frac{l}{W_0\tau} \quad \forall\ 0 \leq l \leq \lceil (m-1)/2 \rceil. \quad (5)$$

The populations of the odd modes are

$$N_{2l-1} = \frac{l}{W_0\tau} \quad \forall\ 0 \leq l \leq \lceil m/2 \rceil. \quad (6)$$

Results from Eqs. (5) and (6) are compared to the numerical results in Fig. 1. We stress that the dependence of the mode occupations on the parity of the level index is a specific feature of bosonic systems that does not appear in the corresponding fermionic cascade [13].

It is also possible to write an equation for the THz emission rate:

$$\frac{dn_{\mathrm{THz}}}{dt} = W_0\sum_{1}^{m} N_k(N_{k-1}+1). \quad (7)$$

Results from Eq. (7) are compared to numerical calculation of the THz emission rate in Fig. 2(a). For high pump powers, the rate increases linearly with the pump power. This represents a limit to the quantum efficiency of THz emission, which is given by the THz emission rate divided by the pump rate, P, and plotted in Fig. 2(b). The presence of the bosonic cascade allows quantum efficiencies exceeding unity and several orders of

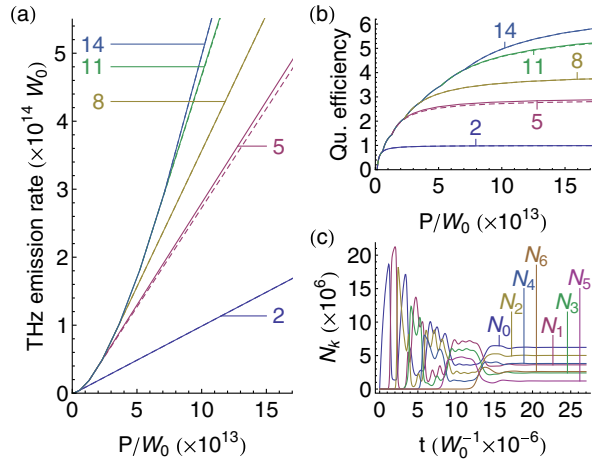

FIG. 2 (color online). (a) Dependence of the THz emission rate on pump intensity in the absence of a cavity for different numbers of modes in the chain (values of m are marked on the plot). Solid curves show results from numerical solutions of Eqs. (1)–(3); dashed curves show the results of Eq. (7) that are valid for high pump powers. (b) Dependence of the quantum efficiency on pump intensity [the values of m are the same as in (a)]. (c) Time dynamics for $m = 6$, $P = 3 \times 10^{13} W$. The parameters are $W_0\tau = 8.3 \times 10^{-7}$ and $n_{\mathrm{THz}} = 0$.

magnitude larger than the quantum efficiency of the corresponding fermionic system. For $W_0\tau \ll 1$, the quantum efficiency of the bosonic cascade reaches $\lceil m/2 \rceil$ at high pump powers. For a fermionic system, cascading does not occur if $W_0\tau \ll 1$, and the quantum efficiency is given by $W_0\tau$ [13].

Figure 2(c) shows the typical time dependence of the mode occupations after the pump is switched on (assumed instantaneously). The enhancement of the scattering via stimulated processes allows the system to reach equilibrium in a time less than $1/W_0$. The presence of multiple dynamically changing effective scattering rates causes an initially chaotic dynamics.

So far, we have considered the stimulated emission of monochromatic but incoherent THz photons. To generate coherent THz photons, an external THz cavity can be considered, where macroscopic numbers of THz cavity photons allow further stimulated enhancement of scattering between the modes. In this case, where upward transitions are allowed in addition to downward ones, the steps observed in Fig. 1 are washed out, as shown in Fig. 3. In contrast to Fig. 1, all modes continue to increase their population with increasing pump power. Figure 4(a) shows the THz emission rate as a function of the THz photon lifetime. For fixed pump intensity, higher THz emission rates are observed than in Fig. 2(a). Figure 4(b) shows the dependence of the THz emission quantum efficiency on the THz photon lifetime. An increase of the THz photon lifetime can increase the quantum efficiency, however, not beyond the limit of $m/2$ already observed in the absence of a THz cavity.

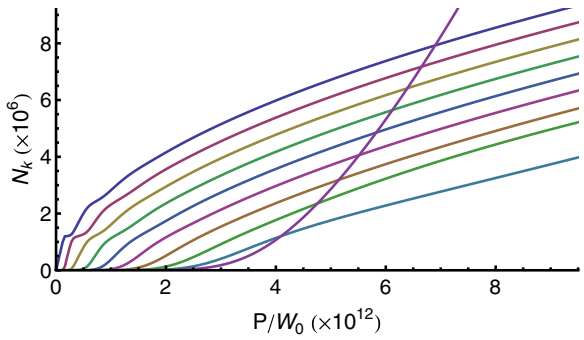

FIG. 3 (color online). Same as in Fig. 1 with a THz cavity. $\tau_{\mathrm{THz}} = \tau/100$.

Let us now demonstrate the feasibility of THz transitions between the size-quantized levels of excitons in a parabolic quantum well. The two-particle Hamiltonian for an electron and a hole reads

$$\mathcal{H} = -\frac{\hbar^2}{2\mu}\frac{\partial^2}{\partial \boldsymbol{\rho}^2} - \frac{e^2}{\epsilon\rho} - \frac{\hbar^2}{2M}\frac{\partial^2}{\partial \boldsymbol{R}^2} + V(z_e, z_h). \quad (8)$$

Here, $M = m_e + m_h$, $\mu = m_e m_h/M$ is the reduced mass of the electron-hole pair, $\boldsymbol{\rho} = \boldsymbol{r}_e - \boldsymbol{r}_h = (x, y, z)$ is the relative coordinate, $\boldsymbol{R} = (m_e\boldsymbol{r}_e + m_h\boldsymbol{r}_h)/M = (X, Y, Z)$ is the center-of-mass wave vector, and ϵ is the background dielectric constant. The quantum well potential $V(z_e, z_h)$ is written in the form $V(z_e, z_h) = A_e z_e^2 + A_h z_h^2$, where constants $A_{e,h}$ denote corresponding stiffness. It is convenient to rewrite $V(z_e, z_h)$ as a function of the center of mass Z and relative motion z coordinates with the result $V = V_0(Z, z) + V_1(Z, z)$, where $V_0(Z, z) = (A_e + A_h)Z^2 + (A_h m_e^2 + A_e m_h^2)z^2/M^2$ does not mix center-of-mass and relative motion and

$$V_1(Z, z) = \frac{2}{M}(m_h A_e - m_e A_h)Zz \quad (9)$$

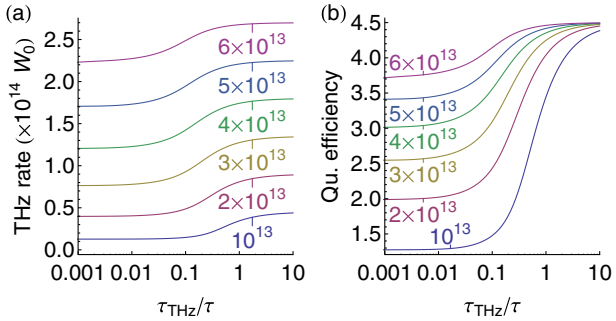

FIG. 4 (color online). (a) Dependence of the THz emission rate in the presence of a THz cavity on the THz photon lifetime. Different curves correspond to different pump powers (marked on the plot in units of W). (b) Dependence of the quantum efficiency on the THz photon lifetime for the same pump powers as in (a). The parameters are $m = 9$ and $W_0\tau = 8.3 \times 10^{-7}$.

mixes internal and center-of-mass degrees of freedom, provided that $m_h A_e \neq m_e A_h$.

In what follows, it is assumed that the potential is weak enough; hence, in the zeroth approximation, the center of mass can be quantized independently and zeroth order wave functions have the form

$$\Psi_{n,l,m,h}(\boldsymbol{r}_e, \boldsymbol{r}_h) = R_{nlm}(\rho) Y_{lm}(\vartheta, \varphi) F_h(Z), \qquad (10)$$

where $F_h(Z)$ are the eigenfunctions of the center-of-mass potential $(A_e + A_h)Z^2$, h enumerates levels in this harmonic potential, $R_{nlm}(\rho)$ are the 3D-hydrogen-like radial functions, and $Y_{lm}(\vartheta, \varphi)$ are (3D) the angular harmonics of relative motion. n, l, and m are the quantum numbers of relative motion of an electron and a hole.

Let us consider the case when the energy of the $2p$ to $1s$ transition of orbital states is matched to the level spacing, $\hbar\Omega$, of the center-of-mass wave functions in the trap [note that V_1 may still be small due to compensation of A_e and A_h terms in Eq. (9)]. The eigenstates of the bosonic cascade can then be written as

$$|\pm, h\rangle = \frac{|1, 0, 0, h\rangle \pm |2, 1, 0, h-1\rangle}{\sqrt{2}}, \qquad (11)$$

where the states are labeled as $|n, l, m, h\rangle$. Dipole transition elements between the two eigenstates at each level in the cascade and those $\hbar\Omega$ lower in energy are given by

$$|\langle \pm, h-1|ex|\pm, h\rangle| = \frac{e}{2}\langle 1, 0, 0, h-1|x|2, 1, 0, h-1\rangle = \frac{64\sqrt{2}}{243} e a_0, \qquad (12)$$

where the numerical factor arises from known matrix elements of transitions in the harmonic oscillator and the hydrogen atom [14,15]. For simplicity, we assume that the populations of $|+, h\rangle$ and $|-, h\rangle$ states in the cascade are equal. The transition rates between different energies in the cascade are then given by the transition rate corresponding to Eq. (12) multiplied by a factor of 2. Following Ref. [4], the transition rate between levels is $W_0 \approx 1700\,\mathrm{s}^{-1}$, where we took $a_0 = 100$ Å and a refractive index of 3 corresponding to a GaAs based system. The $2p$ to $1s$ transition energy was calculated from $E_{np} \approx E_{ns} = -\mathcal{R}/n^2$, with $\mathcal{R} = 5$ meV. Taking $\tau = 500$ ps, we then have $W_0\tau \approx 8.3 \times 10^{-7}$.

We have neglected any energy splitting of the eigenstates $|\pm, h\rangle$, which is valid if the coupling energy given by V_1 is less than the inhomogeneous broadening of the system. Note that the $|\pm, h\rangle$ are still the unique eigenstates of the system, provided that the coupling energy exceeds the decay rate given by the exciton lifetime.

To best characterize the specific case of a parabolic trap with electron-hole mixing, we have also considered the effects of higher order transitions [13] caused by the mixing of states by $V_1(Z, z)$. Dipole transitions between next-nearest-neighbor levels are forbidden; however, third order transitions between next-next-nearest-neighbor levels are possible [13]. In addition, we have considered the effect of exciton-exciton scattering processes [13]. The results are summarized in Fig. 5. The exciton-exciton interactions can greatly smooth the quantized steps, while the influence of first and third order transitions may distort the differences in populations of neighboring levels. However, the parity dependence can still be observed as nontrivial oscillations of the level populations with increasing power.

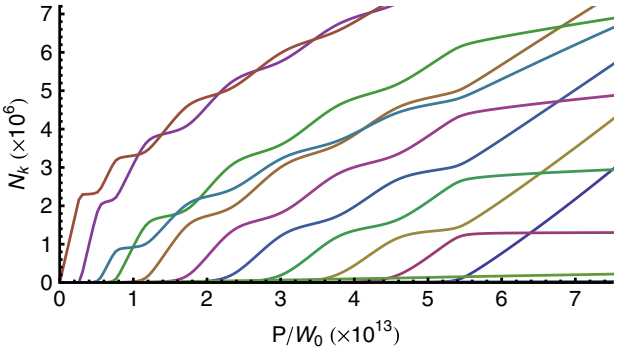

FIG. 5 (color online). Same as in Fig. 1, including exciton-exciton scattering [13] and corrections to transition rates up to third order in V_1 (fourth order corrections vanish).

Furthermore, high quantum efficiencies, exceeding unity, are still possible [13] due to the weakness of third order transitions and the fact that exciton-exciton pair scattering conserves energy. Note, the number of THz photons that a pair of excitons can emit before reaching the ground state is unchanged even if exciton-exciton scattering takes place.

Finally, we note that the wave guiding geometry can increase the active volume of the laser and, consequently, the output power. Its drawback is a larger size compared to the vertical cavity laser geometry. Lateral traps would allow a more compact size of the device, while the matrix elements of terahertz transitions are believed to be larger in parabolic quantum wells.

In summary, we proposed the use of a bosonic cascade to implement THz lasing with high quantum efficiency, above unity. Such a device requires a parabolic trapping that can be arranged in the plane of a semiconductor microcavity via a variety of techniques or using parabolic wide quantum wells. The THz transition matrix elements were calculated, making use of possible resonance between the level spacing of center-of-mass wave functions and the $2p$ to $1s$ transition energy. A series of steps in the mode occupations of the bosonic cascade was predicted for increasing pump power, which remain as visible oscillations in the presence of exciton-exciton scattering and third order transitions.

This work has been supported by the EU IRSES projects "POLAPHEN" and "POLATER." I. A. S. acknowledges the support from Rannis "Center of Excellence in Polaritonics." M. M. G. was partially supported by the RFBR and RF President Grant No. NSh-5442.2012.2. M. A. K. acknowledges the RFBR.

[1] R. F. Kazarinov and R. A. Suris, Sov. Phys. Semicond. **5**, 707 (1971).
[2] J. Faist, F. Capasso, D. L. Sivco, C. Sirtori, A. L. Hutchinson, and A. Y. Cho, Science **264**, 553 (1994).
[3] E. Normand and I. Howieson, Laser Focus World **43**, 90 (2007).
[4] K. V. Kavokin, M. A. Kaliteevski, R. A. Abram, A. V. Kavokin, S. Sharkova, and I. A. Shelykh, Appl. Phys. Lett. **97**, 201111 (2010).
[5] I. G. Savenko, I. A. Shelykh, and M. A. Kaliteevski, Phys. Rev. Lett. **107**, 027401 (2011).
[6] A. V. Kavokin, I. A. Shelykh, T. Taylor, and M. M. Glazov, Phys. Rev. Lett. **108**, 197401 (2012).
[7] D. Bajoni, E. Peter, P. Senellart, J. L. Smirr, I. Sagnes, A. Lemaître, and J. Bloch, Appl. Phys. Lett. **90**, 051107 (2007).
[8] R. Bailili, V. Hartwell, D. Snoke, L. Pfeiffer, and K. West, Science **316**, 1007 (2007).
[9] A. Amo, S. Pigeon, C. Adrados, R. Houdré, E. Giacobino, C. Ciuti, and A. Bramati, Phys. Rev. B **82**, 081301(R) (2010).
[10] E. Wertz, L. Ferrier, D. D. Solnyshkov, R. Johne, D. Sanvitto, A. Lemaître, I. Sagnes, R. Grousson, A. V. Kavokin, P. Senellart, G. Malpuech, and J. Bloch, Nat. Phys. **6**, 860 (2010).
[11] G. Tosi, G. Christmann, N. G. Berloff, P. Tsotsis, T. Gao, Z. Hatzopoulos, P. G. Savvidis, and J. J. Baumberg, Nat. Phys. **8**, 190 (2012).
[12] L. E. Golub, A. V. Scherbakov, and A. V. Akimov, J. Phys. Condens. Matter **8**, 2163 (1996).
[13] See Supplemental Material at http://link.aps.org/supplemental/10.1103/PhysRevLett.110.047402 for the analytic solutions to the rate equations in the bosonic and fermionic cases, calculation of higher order terms in the perturbation expansion, calculation of exciton-exciton scattering terms, and consideration of a system in thermal equilibrium.
[14] L. Landau and E. Lifshitz, *Quantum Mechanics: Non-Relativistic Theory* (Butterworth-Heinemann, Oxford, 1977), Vol. 3.
[15] V. B. Berestetskii, L. P. Pitaevskii, and E. M. Lifshitz, *Quantum Electrodynamics* (Butterworth-Heinemann, Oxford, 1999), 2nd ed., Vol. 4.